Accredited Ranking SINTA 2
Decree of the Director-General of Higher Education, Research, and Technology, No. 158/E/KPT/2021
Validity period from Volume 5 Number 2 of 2021 to Volume 10 Number 1 of 2026

Published online on: **http://jurnal.iaii.or.id**

JURNAL RESTI
(Rekayasa Sistem dan Teknologi Informasi)
Vol. 6 No. 5 (2022) 782 - 789 ISSN Media Electronic: 2580-0760

Surrogate Model-based Multi-Objective Optimization in Early Stages of Ship Design

Nanda Yustina[1], Ari Saptawijaya[2]
[1,2] Department of Computer Science, Faculty of Computer Science, Universitas Indonesia, Depok, Indonesia
[1]Research Center for Transportation Technology, Badan Riset dan Inovasi Nasional, Tangerang Selatan, Indonesia
[1]nanda.yustina@ui.ac.id, [2]saptawijaya@cs.ui.ac.id

Abstract

The abstract isthe early stages of ship design, the decision of the ship's main dimensions significantly impacts the ship's performance and the total cost of ownership. This paper focuses on an optimization approach based on surrogate models at the early stages of ship design. The objectives are to minimize power requirements and building costs while still satisfying the constraints. We compare three approaches of surrogate models: Kriging, BPNN-PSO (Backpropagation Neural Network-Particle Swarm Optimizer), and MLP (Multi-Layer Perceptron) in two multi-objective optimization algorithms: MOEA/D (Multi-Objective Evolutionary Algorithm Decomposition) and NSGA-II (Non-Dominated Sorting Genetic Algorithm II). The experimental results show that MLP surrogate models get the best performance with MAE 6.03, and BPNN-PSO gets the second position with MAE 7.2. BPNN-PSO and MLP with MOEA/D and NSGA-II improve the design with around 58% smaller adequate power and 6% less steel weight than the original design. However, BPNN-PSO and MLP have lower hypervolume than Kriging for both optimization algorithms MOEA/D and NSGA-II. On the other hand, Kriging has the most inadequate model accuracy performance, with an MAE of 22.2, but produces the highest hypervolume, lowest computational time, and far lower objective values than BPNN-PSO and MLP for both optimization algorithms, MOEA/D and NSGA-II. Nevertheless, the three surrogate model approaches can significantly improve ship design solutions and reduce work time in the early stages of design.

Keywords: ship design, multi-objective optimization, surrogate model, neural network, particle swarm optimizer

1. Introduction

The growing competitiveness of the shipping sector as a result of digitalization and rules from the International Maritime Organization (IMO) to decrease CO2 emissions requires ship design solutions to be created with shorter lead times and a lower Energy Efficiency Design Index (EEDI) (the time between the initiation and completion of a production process) [1]. The ship's EEDI is proportional to the power required; thus, naval architects try to minimize the ship's power requirements in every possible way to reduce the ship's carbon emissions [2]. Aside from the environmental objective, naval architects should ensure that the design can fulfill the ship owner's requirements while meeting the applicable regulations [3].

Calculating total cost ownership is equally essential but rarely explained further in ship design. The total cost of ownership for ships generally consists of building costs (CAPEX) and operational costs (OPEX). Building costs are strongly affected by material costs, and the required steel weight can represent them. Meanwhile, operating costs are affected by ship speed and moved cargo, which defines ship power requirements and further affects fuel consumption. Therefore, minimizing the need for ship power and steel weight can reduce the total cost of ownership [4].

Conventionally, the ship design process is divided into four phases, from concept design to detailed design, as described in the Design Spiral concept (Figure 1). In the early stages, concept design translates the ship owner's requirements into fundamental elements of the proposed method, such as estimating the ship's dimensions, construction weight, building costs, and performance. In this design spiral concept, an iterative process of sequential design work sections is employed to optimize the design components [3]. However, this approach is very time-consuming. Furthermore, since naval architects cannot consider all dependencies between decision variables, constraints, and objectives, the design process will likely lead to the local optima

Accepted: 06-07-2022 | Received in revised: 10-09-2022 | Published: 31-10-2022

solution. Hence, there is no guarantee of achieving optimal design from the point of view of each discipline [4].

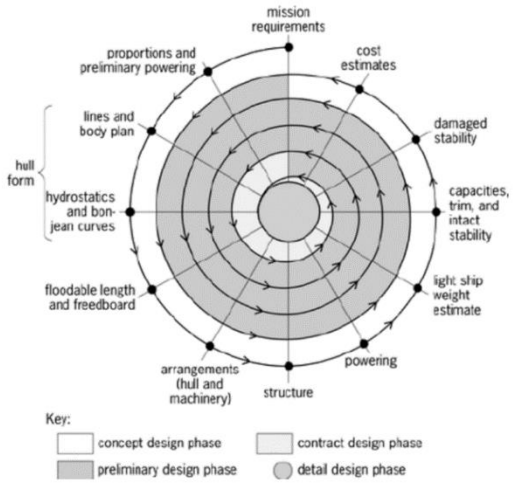

Figure 1. Classical Ship Design Spiral

The ship's dimensions have a significant impact on assessing the ship's power requirement and building cost. Optimizing the ship's measurements in the early stages of ship design is preferable since the effort for the early stages is relatively low [5].

Surrogate model-based optimization is one approach to optimization problems. A surrogate model approximates the input-output data obtained from a simulation. Once the surrogate model is trained using input-output data, analytical representations of the constraints and objectives of the black-box problem become available, and it is computationally cheaper to evaluate [6]. Therefore, a surrogate model replacing the time-consuming process of ship design simulations is highly appreciated.

Previous studies have mainly performed optimization with machine learning approaches for a single objective of ship design. Li (2014) performed optimization of ship resistance using an approximation approach based on Support Vector Regression (as a surrogate model) in the optimization [7]. Jafaryeganeh (2020) determined an internal layout design of the ship with the Pareto optimal set [8]. Abramowski (2013) built a neural network model to calculate adequate power and optimize it using a Genetic Algorithm [9]. The use of multi-objective optimization based on the surrogate model approach in ship design has been shown by De Winter (2019). CEGO [3] is used for multi-objective optimization, where Kriging is employed as a surrogate model for objectives function and Cubic Radial Basis Functions (CRBF) as a surrogate model for constraints function. Later, the feasible solution was selected by using S-metric multi-objective optimization. While De Winter optimized the next iteration of the dredger design, which was first set up in the ACD framework[1] by naval architects [3], this study focuses differently on the early stages of ship design, namely for a type of vessel: tanker ships.

Other studies focus on other areas of engineering design. In antenna structure design, Qin (2018) used Backpropagation Neural Networks – Particle Swarm Optimizer (BPNN-PSO) as a surrogate model for Multi-Objective Evolutionary Algorithms Decomposition (MOEA/D) [10]. As for the result, the proposed approach can provide higher accuracy and lower optimization time than other existing antenna structure optimization methods. In nuclear engineering, Whyte (2020) applied deep learning methods, MLP, and CNN as surrogate models for optimizing the design of a 'micro core' simulation [11]. As for the results, surrogate models can accelerate optimization at the start of the process.

In this study, we compare three approaches of the surrogate models that have been proven to solve multi-objective problems in their respective fields: Kriging [3]; Backpropagation – particle swarm optimizer (BPNN-PSO) [10]; and Multi-layer Perceptron (MLP) [11]. We evaluate the surrogate models in two multi-objective optimization algorithms: MOEA/D [12] and NSGA-II [13]. This study has two design objectives: minimizing power requirements and shipbuilding costs while still satisfying various constraints.

There are two main contributions to this paper. First, we apply different surrogate model-based multi-objective optimization in the early stages of ship design with two objectives, to minimize both power requirements and shipbuilding costs. Since this study also evaluates three surrogate model approaches and two optimization problems, the second contribution is the result that provides new insights for performance measures in multi-objective optimization.

The next part of the paper is organized as follows. Section II explains the research methods that describe problem formulations, stages, and scenarios used in the experiments. Section III presents the experiment result and its discussion. Finally, Section IV concludes the paper and suggests some future work.

2. Research Methods

This study compares three surrogate models and two optimization algorithms to solve a ship design optimization problem. First, we describe the

[1] Accelerated Concept Design (ACD) framework is a commercially used software from C-Job Naval Architects, 2019. https://c-job.com/

DOI: https://doi.org/10.29207/resti.v6i5.4248

formulation of the optimization problem. Then, we explain the research stages.

2.1 Ship Design Optimization Problem

Generally, the multi-objective ship design optimization can be stated as a Multi-objective Problem (MOP),

$$\min_{\vec{x}} \vec{f}(\vec{x}) \quad \text{where} : \vec{f}(\vec{x}) = [f_1(\vec{x}), \dots, f_k(\vec{x})] \qquad (1)$$

where $\vec{f}$ is a vector function, which has k design objective, and $\vec{x}$ is a decision variable vector. A decision variable vector $\vec{x}$ consists of n variables, $\vec{x} = [x_1, \dots, x_n]$ and is part of the feasible solution $\vec{x} \in \Omega$. The feasible region Ω contains all solutions that satisfy some given constraints, including the bounds of variables and inequality constraints [3] [14]:

$$x_i^{lower} \leq x_i \leq x_i^{upper} \qquad i = \{1, \dots, n\} \qquad (2)$$

$$g_i(\vec{x}) \leq c_i \ \vee \ g_i(\vec{x}) \geq c_i \quad i = \{1, \dots, m\} \qquad (3)$$

The bounds of variables define the minimum and maximum values for each x in the decision variables $\vec{x}$. As for inequality constraints, g_i represents one of the m constraints, which is a generally non-linear, real-valued function of the decision variables $\vec{x}$ and a constant value c_i.

2.1.1 Decision Variables

The decision variables of a ship design problem are the numerical quantities whose values can be varied in the optimization process [3]. These quantities are denoted as x_j , where j = 1, ..., n, and x_j represents one decision variable. The vector $\vec{x}$ consists of n variables are then represented by $\vec{x} = [x_1, \dots, x_n]$. In this study, there are five continuous variables of the ship's main dimension: length perpendicular (L), Breadth (B), Height (H), Draught (T), and Speed (V).

2.1.2 Objective Functions

The problem in this study is the minimization problem, where the best solution is the solution with the lowest possible objective function value. This ship design case has two objectives: minimizing power requirements as f_1, and steel weights as f_2. While the two objectives may appear to be a minimization problem, they are a classic example of conflicting goals. When the solution obtains the lowest possible value for the objective function f_i, the value of another objective function, f_j, would be higher and vice versa [14] [15]. In ship design problems, longer and leaner ships will lead to lower hull resistance, resulting in more efficient powering requirements. However, they will have higher steel weight, resulting in higher shipbuilding costs. On the other hand, shorter ship widths will have higher hull resistance but lower steel weight, resulting in less efficient powering requirements but lower shipbuilding costs [3]. Therefore, the solution for a multi-objective problem is a set of solutions and not a single point [14]. The solutions, called Pareto-optimal set $\mathcal{P}$, are decision variable vectors in the feasible set non-dominated by other vectors. We define the non-dominated relation $\prec$ for the two design variable vectors $\vec{u}$ and $\vec{v}$, as $\vec{u} \prec \vec{v}$ ($\vec{u}$ dominates $\vec{v}$) if $f_k(\vec{u}) \leq f_k(\vec{v})$ for all $k = \{1, \dots, m\}$ and $f_k(\vec{u}) < f_k(\vec{v})$ for at least one k [3] [16]. In other words, a solution $\vec{u}$ dominates another solution $\vec{v}$, if and only if $\vec{u}$ is better or equal in all objectives and strictly better in at least one objective. When each solution in the Pareto-optimal set is mapped into the objective functions $\vec{f}(\vec{x})$, they will create the Pareto-front PF. With the Pareto-front, the engineer can visualize the consequences of the decision on each objective to be achieved.

2.1.3 Constraints

Generally, the constraints of a ship design optimization problem can be divided into two categories, domain constraints given by the regulating authorities and physical constraints provided by the client. In this study, the constraints used are domain constraints: the bounds of variable and inequality constraints related to decision variables, as stated in Equations 2 and 3. These variables' bounds are obtained based on a real dataset of tanker ships with a deadweight tonnage (DWT) of 4500 – 5500 tonnes. The inequality constraints are suggested values of coefficients connected to the ship's principal dimensions to assure the strength of a hull and stability standards. Such as the recommendations limiting the Froude Number (Fn) for tanker ships, L to B, B to T, L to T, and D to T [17]. of the Froude Number (Fn) for tanker ships, L to B, B to T, L to T, and D to T [17]. Moreover, constraints are used to verify the initial dataset and each individual in the population generated by the evolutionary algorithm. Therefore, the optimum values of objectives design can either occur at the boundaries of the constraints or between them. The ranges for variables bound and inequality constraints used in this study can be seen in Table 1.

Table 1. Constraints ranges used in this study

Constraints	Ranges
Variables bound	$80 \leq L \leq 130$
	$10 \leq B \leq 25$
	$5 \leq D \leq 15$
	$3 \leq T \leq 10$
	$14 \leq V \leq 18$
Froude Number (Fn)	$Fn \leq 0.32$
L/B	$3.5 \leq L/B \leq 10$
B/T	$1.8 \leq B/T \leq 5$
L/T	$10 \leq L/T \leq 30$
L/D	$L/D \leq 15$

2.2 Research Stages

As shown in Figure 2, the research consists of several stages: generating the initial dataset, validating the dataset and getting the response set, constructing

DOI: https://doi.org/10.29207/resti.v6i5.4248

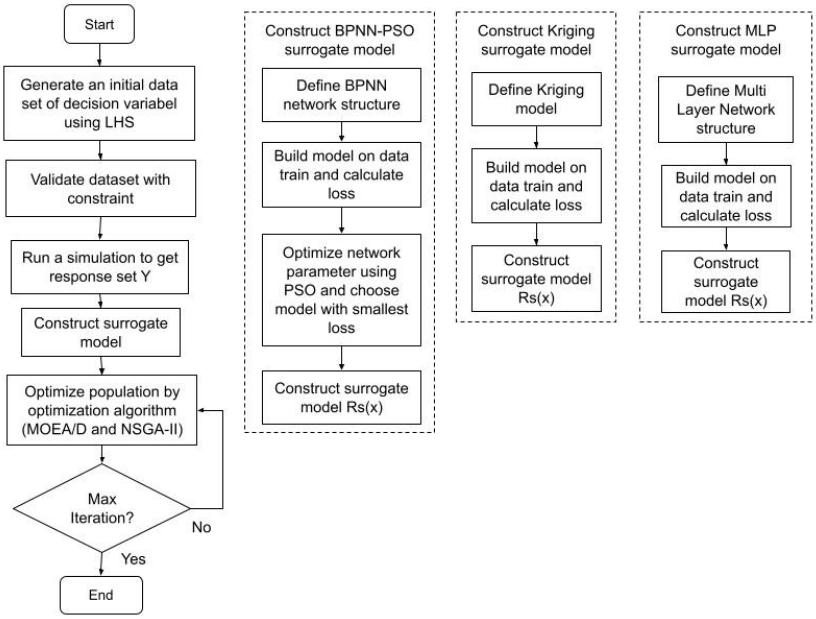

Figure 2. Research Stages Flowchart

surrogate models, and optimizing the population by optimization algorithms.

2.2.1. Generate Initial Dataset

The first stage begins by creating a dataset in a design space rather than using actual data of the ship's main dimension. The dataset consists of decision variables obtained by generating design space using Latin Hypercube Sampling (LHS) [3] [10] to ensure that generated samples are as uncorrelated as possible. This way, LHS can maximize the average amount of information gained by computing the objectives and constraints. The recommended minimum size of the LHS is $11.n-1$, where n is the number of decision variables [3]. In this study, the size of the initial dataset is 150, divided into 80:20 for training and testing data, respectively. As mentioned previously, the dataset from the design space is limited by the variable bounds in Table 1.

2.2.2. Validate Dataset and Get Response Set Y

Next, we acquire response set Y for each data point using manual simulations. A manual simulation is a step-by-step calculation performed manually by naval engineers. As explained in the spiral design concept above, this manual simulation is usually time-consuming. A naval architect takes days to collect data and perform manual simulations for initial calculations. Later, the obtained data (decision variables with their corresponding response set) are trained by using three different surrogate models separately: BPNN-PSO, Kriging, and MLP.

2.2.3. BPNN-PSO

In this surrogate model, PSO is used to optimize the network parameters of BPNN. The BPNN topology is shown in Figure 3 [10]. Particles from PSO represent each connection weight and bias of BPNN, so the dimension of particles are calculated using:

$$d = n_{inp} \times n_h + n_h \times n_{out} + n_h + n_{out} \quad (4)$$

where n_{inp} is the number of inputs (the number of design variables), n_h is the number of the hidden nodes, and n_{out} is the number of outputs. Later, the particles are optimized using the formula:

$$find\ \mathcal{Z}_{op} = \arg\min_{z} f(z)$$
$$such\ that\ z \in (0,1)^d \quad (5)$$

where $z = [z_0, \dots, z_d]$ is a PSO particle, $\mathcal{Z}_{op}$ is optimal positions of particles, and $f(z)$ is the scalar fitness function for the neural network to minimize the mean square error (MSE).

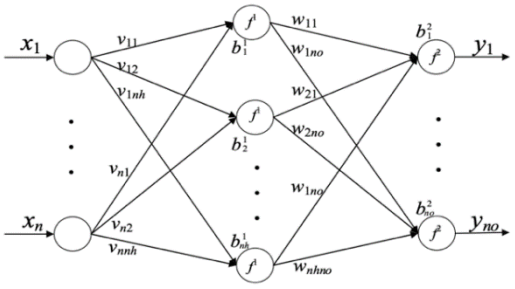

Figure 3. The topology of a three-layer BPNN

2.2.4. Kriging

Kriging, or the Gaussian Process Regression model, is a generic supervised learning method that calculates the probability distribution over all admissible functions that fit the data. This Gaussian Process is defined by a mean function $m(x)$ and positive definite covariance function $k(x, x')$ [18]:

DOI: https://doi.org/10.29207/resti.v6i5.4248

$$f(x) \sim \mathcal{GP}\big(m(x), k(x,x')\big) \quad (6)$$

jointly Gaussian with zero mean and covariance given by:

$$k(x,x') = \exp\left(-\frac{1}{2}|x-x'|^2\right) \quad (7)$$

where x and x' represent values in the input space. In this case, the mean is 0, as it is assumed that there is no noise in the data.

2.2.5. MLP

MLP is a fully connected multi-layer perceptron commonly used for regression and classification tasks. The topology of MLP is similar to that of Figure 3, except that it may be constituted by more than one hidden layer. Each node connects inputs x to outputs y; each node sums the inputs and applies the weighting factor$w_{i,j}$ and transforms to the data. Then the backpropagation algorithm is used to update the weights of the network [11]. After the training, the final weights are defined as an approximating output. In this study, we use five hidden layers for MLP, with 60 hidden nodes for each hidden layer and two output layers.

2.2.6. Construct Surrogate Models

K-fold cross-validation with K=5 is used in the training process to evaluate the models. The best model is obtained by calculating the mean absolute error (MAE) for each fold of the validation set.

2.2.7. Optimize Population

Finally, we populate and evolve data using MOEA/D with each Surrogate Model. NSGA-II is also used to compare the results. MOEA/D is an evolutionary algorithm (EA) by Zhang (2007) that decomposes a multi-objective optimization problem into several scalar optimization subproblems and optimizes them simultaneously [12]. On the other hand, NSGA-II [13] uses a non-dominated sorting-based selection operator to create a mating pool by combining the parent and child population to select the best N solutions for the next generation.

Every individual generated in the population is also verified using the given constraint. Experiments were carried out for each surrogate model, with different numbers of population: 100 and 200. Each population evolves into three generations: 50, 100, and 200.

Hypervolume (HV) is used to evaluate the optimization results. A hypervolume is an area between a fixed reference point and the Pareto front, used as an indicator of the quality of a set of solutions that are not dominated by other solutions (Pareto fronts) in a multi-objective problem, as illustrated in Figure 4 [3]. A Reference Point can be obtained from a fixed point dominated by all points in the set of effectiveness [14]. From that definition, the higher HV can indicate that the algorithm performs better for the problem. The reference point in this study is fixed and set to [2000, 1200]. This reference point means we do not allow the algorithm to find solutions with a power requirement exceeding 2000 kW or a steel weight higher than 1200 tonnes.

Besides HV, the spread of the Pareto front is also considered. This spread is the distribution of the points along Pareto front approximations. A smaller distance between points in Pareto front approximations indicates better-distributed solutions [15].

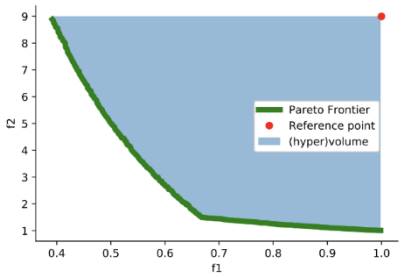

Figure 4. Illustration of hypervolume indicator

3. Results and Discussions

This section discusses the experiment results, from surrogate model accuracy to optimization results.

3.1 Surrogate Model Accuracy

As previously explained, the size of the initial dataset is 150, divided into 80:20 for the training and test data. The loss function used in this experiment is the MAE. As shown in Table 2, the validation score is the mean score obtained from each fold in cross-validation, and the test score is obtained from the prediction score of test data. MLP gets the best performance, represented by the most petite MAE for the validation and test data, respectively 4.09 and 6.03. BPNN PSO has a slightly lower performance than MLP, with the MAE for validation data being 7.9 and the test data being 7.2. Kriging performs inadequately more than the other two models, with MAE 22.2 for validation data and 22.9 for test data.

Table 2. Mean Absolute Error (MAE) for Validation and Test Data

Model	Validation MAE	Test MAE
Kriging	22.2	22.9
BPNN-PSO	7.9	7.2
MLP	4.09	**6.03**

3.2 Optimization Results

Table 3 shows the optimization results comparing three surrogate models using MOEA/D and NSGA-II, respectively. These results indicate that Kriging provides the highest value for hypervolume and the fastest computational time. Kriging produces a hypervolume value almost twice greater than BPNN-

DOI: https://doi.org/10.29207/resti.v6i5.4248

PSO and MLP, both when using MOEA/D and NSGA-II. In optimization with MOEA/D, BPNN-PSO has higher hypervolume than MLP in a small population. Meanwhile, in NSGA-II, MLP produces higher hypervolume than BPNN-PSO for all populations and generations.

Table 3. Hypervolume of the non-dominated solution and computational time (in Second) using MOEA/D and NSGA-II

Pop/ Gen	Surrogate Model					
	Kriging		BPNN-PSO		MLP	
	HV	Time	HV	Time	HV	Time
MOEA/D						
100/50	800.7	26.7	432.1	33.3	429.3	182
100/100	800.9	53.1	433.3	65.8	430.2	424
100/200	800.9	133	433.4	165	430.5	1056
200/50	790.6	67	434.2	89	434.4	533
200/100	790.6	134	434.8	177	435.1	1012
200/200	790.6	340	434.9	400	435.1	2158
NSGA-II						
100/50	800.8	28	409.6	38	412.3	266
100/100	800.8	54.6	409.6	75	417.8	673
100/200	800.8	132	409.6	165	417.8	1458
200/50	800.8	54	409.6	89	417.8	342
200/100	800.8	107	409.6	177	430.9	692
200/200	800.8	265	409.6	400	430.9	1384

However, Kriging and BPNN-PSO surrogate models on both MOEA/D and NSGA-II did not provide a larger hypervolume when increasing the population and generation. Meanwhile, MLP still increases hypervolume, even though the computational time is about an order of magnitude larger than Kriging and BPNN-PSO, both using MOEA/D and NSGA-II. For optimization algorithm comparison, MOEA/D gives better hypervolume results than NSGA-II for BPNN-PSO and MLP. Meanwhile, Kriging has different outcomes. It gets higher hypervolume when optimized by NSGA-II.

Figure 5 shows the distribution of the initial population evaluation, and the Pareto front for each surrogate model and optimization algorithm are visualized. In Figures 5b and 5c, the combination of MOEA/D with BPNN-PSO and MLP results in smaller distances between points in Pareto front approximations. In Figures 5e and 5f, the combination of NSGA-II with BPNN-PSO and MLP results in a more significant distance between the facts, but the distribution still looks uniform when MOEA/D is used.

For the objective values, we can see from these figures that f_1, and f_2 have contradictory values. When the solution obtains the lowest possible value for the objective function f_1, the value of the objective function f_2 would be higher, and vice versa. In Figures 5b and 5c, BPNN-PSO and MLP combined with MOEA/D have these contradictory values for f_1 and f_2 in the Pareto front, as well as BPNN-PSO and MLP, combined with NSGA-II in Figures 5e and 5f. The original design has a power requirement of 1290 kW for f_1 value and steel weight of 992 tonnes for f_2 value, marked in red in Figure 5. Meanwhile, the MLP Pareto front with MOEA/D and NSGA-II in Figures 5c and 5f are contradictory when their f_1 values are 1340 and 1385, respectively, and f_2 reached their minimum, 819 and 831, respectively. These f_1 values are slightly higher than the f_1 deal with the original design. At the same time, BPNN-PSO Pareto front with MOEA/D and NSGA-II in Figures 5b and 5e have f_1 values of 1703 and 1614, respectively, when f_2 went to its minimum, namely 753 and 761.

Moreover, when we compare objective values to the expert's original design, each optimization result has the most interesting minimized objectives in their Pareto front design variation, marked in blue in Figure 5. MOEA/D with BPNN-PSO has a marked f_1 value of 533 kW and an f_2 weight of 956 tonnes. At the same time, MOEA/D with MLP has a close marked f_1 value of 519 kW and an f2 value of 926 tonnes. NSGA-II with BPNN-PSO and MLP give the same pattern. NSGA-II with BPNN-PSO has a marked f_1 value of 532 kW and an f_2 value of 945 tonnes, while NSGA-II with MLP has 519 kW for f_1 value and 926 tonnes for f_2 value. Therefore, the marked objective values of BPNN-PSO and MLP for both optimization, MOEA/D, and NSGA-II, improve the design with around 58% smaller adequate power and 6% less steel weight than the original design. Afterward, even though BPNN-PSO and MLP have equally lower hypervolume for optimization, they have adequate model accuracy performance (MAE).

On the other hand, Kriging has the lowest model accuracy performance but has the highest hypervolume. MOEA/D with Kriging has marked f_1 value in Pareto Front of 484 kW and the f_2 value of 813 tonnes. Meanwhile, NSGA-II with Kriging has 366 kW for f_1 value and 796 tonnes for f_2 value. Compared to the original design, the marked objective values of Kriging with MOEA/D and NSGA have around 62% smaller effective power and 18% less steel weight. However, these values are far lower than BPNN-PSO and MLP, as well as the original design. The data spread in figures 5a and 5d also look different compared to BPNN-PSO and MLP for both MOEA/D and NSGA-II. They also have a more considerable distance between points in Pareto front approximations. It could happen because the model error affects the lowest objective value, thus affecting the hypervolume value. Therefore, hypervolume cannot be the only performance metric for optimization with the surrogate model approach.

DOI: https://doi.org/10.29207/resti.v6i5.4248

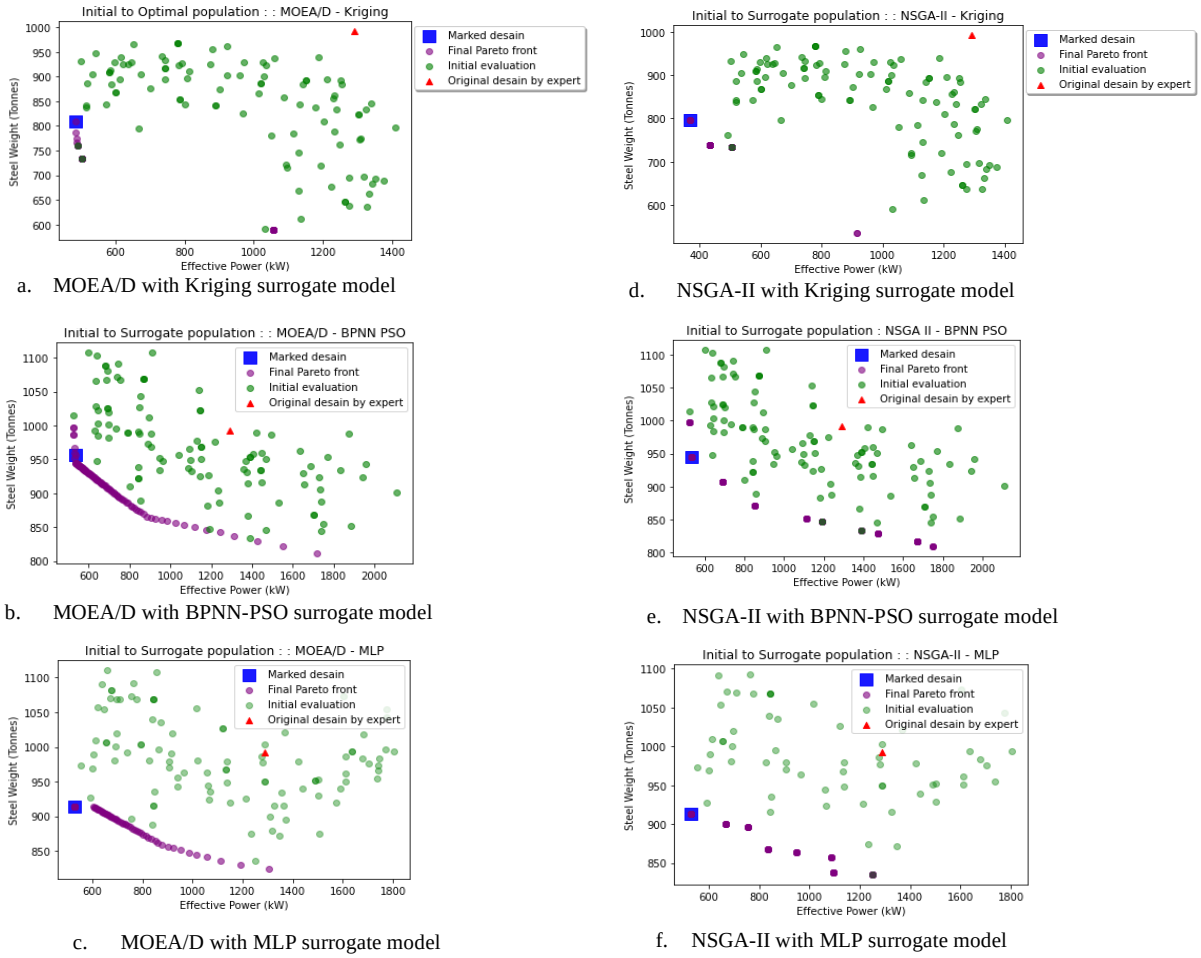

a. MOEA/D with Kriging surrogate model

d. NSGA-II with Kriging surrogate model

b. MOEA/D with BPNN-PSO surrogate model

e. NSGA-II with BPNN-PSO surrogate model

c. MOEA/D with MLP surrogate model

f. NSGA-II with MLP surrogate model

Figure 5. Pareto frontier obtained by Kriging, BPNN-PSO, and MLP Surrogate model on MOEA/D and NSGA-II

Nevertheless, hypervolume can still measure performance between optimization algorithms with the same surrogate model.

4. Conclusion

In this study, three surrogate models: Kriging, BPNN-PSO, and MLP, have been employed for multi-objective optimization in the early stages of the ship design problem. MLP surrogate models get the best performance with MAE 6.03, while BPNN-PSO gets the second position with MAE 7,2. These two MAE results have around three times lower than Kriging. Kriging has the most down computational time, 28 seconds. In comparison, MLP has the longest computational time, namely 23 minutes. Therefore, that indicates that the surrogate model can replace manual simulations that are usually carried out manually by the naval expert, which takes days.

For optimal results, each combination of surrogate model and optimization algorithm has the most interesting minimized objectives in their Pareto front design variation compared to the expert's original design. The significant objective values of BPNN-PSO and MLP for both optimizations, MOEA/D and NSGA-II, improve the design with around 58% smaller adequate power and 6% less steel weight than the original design. BPNN-PSO and MLP also have a better spread on the approximation of the Pareto front than Kriging for both optimization algorithms, MOEA/D and NSGA-II. Meanwhile, Kriging, which has the lowest model accuracy performance, produces the highest hypervolume and far lower objective values than BPNN-PSO and MLP for both optimization algorithms, MOEA/D and NSGA-II. It could happen because the model error affects the lowest objective value, thus affecting the hypervolume value. Therefore, hypervolume cannot be the only performance metric for optimization with the surrogate model approach. Nevertheless, hypervolume can still measure performance between optimization algorithms as long as they have the same surrogate model.

For future work, it is interesting to study how to increase neural network-based surrogate model accuracy with lower computational time. At the same time, explore other evaluation metrics for surrogate model-based multi-objective algorithms to apply them in this problem domain.

DOI: https://doi.org/10.29207/resti.v6i5.4248

Acknowledgments

This work is supported by BRIN (Indonesian National Research and Innovation Agency) Education and Training Center under SAINTEK Scholarship. We also thank Dr. Ir. Iskendar, MS., and Noor Mohammad Ridha Fuadi, S.T., for their help in problem identification as naval experts and their assistance in data acquisition.

Reference

[1] N. D. Charisi *et al.*, "Parametric Modelling Method based on Knowledge Based Engineering: The LNG Bunkering Vessel Case," 2020, p. 17.

[2] S. Chakraborty, "How The Power Requirement Of A Ship Is Estimated?" Accessed: Feb. 05, 2021. [Online]. Available: https://www.marineinsight.com/naval-architecture/power-requirement-ship-estimated/

[3] R. de Winter, B. van Stein, M. Dijkman, and T. Bäck, "Designing Ships Using Constrained Multi-objective Efficient Global Optimization," Springer International Publishing, Cham, 2019. doi: 10.1007/978-3-030-13709-0_16.

[4] R. de Winter, J. Furustam, T. Bäck, and T. Muller, "Optimizing Ships Using the Holistic Accelerated Concept Design Methodology," in *Practical Design of Ships and Other Floating Structures*, Singapore, 2021, vol. 65, pp. 38–50. doi: 10.1007/978-981-15-4680-8_3.

[5] A. Charchalis, "Determination Of Main Dimensions And Estimation Of Propulsion Power Of A Ship," *J. KONES Powertrain Transp.*, vol. 21, no. 2, 2014, doi: 10.5604/12314005.1133863.

[6] S. H. Kim and F. Boukouvala, "Machine learning-based surrogate modeling for data-driven optimization: a comparison of subset selection for regression techniques," *Optim. Lett.*, vol. 14, no. 4, pp. 989–1010, Jun. 2020, doi: 10.1007/s11590-019-01428-7.

[7] D. Li, P. A. Wilson, Y. Guan, and X. Zhao, "An Effective Approximation Modeling Method for Ship Resistance in Multidisciplinary Ship Design Optimization," in *Volume 2: CFD and VIV*, San Francisco, California, USA, Jun. 2014, p. V002T08A023. doi: 10.1115/OMAE2014-23407.

[8] H. Jafaryeganeh, M. Ventura, and C. Guedes Soares, "Application of multi-criteria decision making methods for selection of ship internal layout design from a Pareto optimal set," *Ocean Eng.*, vol. 202, p. 107151, Apr. 2020, doi: 10.1016/j.oceaneng.2020.107151.

[9] T. Abramowski, "Application of Artificial Intelligence Methods to Preliminary Design of Ships and Ship Performance Optimization," *Nav. Eng. J.*, p. 13, 2013.

[10] W. Qin, J. Dong, M. Wang, Y. Li, and S. Wang, "Fast Antenna Design Using Multi-Objective Evolutionary Algorithms and Artificial Neural Networks," in *2018 12th International Symposium on Antennas, Propagation and EM Theory (ISAPE)*, Hangzhou, China, Dec. 2018, pp. 1–3. doi: 10.1109/ISAPE.2018.8634075.

[11] A. Whyte and G. Parks, "Surrogate Model Optimization Of A 'Micro Core' Pwr Fuel Assembly Arrangement Using Deep Learning Models," p. 8, 2020.

[12] Qingfu Zhang and Hui Li, "MOEA/D: A Multiobjective Evolutionary Algorithm Based on Decomposition," *IEEE Trans. Evol. Comput.*, vol. 11, no. 6, pp. 712–731, Dec. 2007, doi: 10.1109/TEVC.2007.892759.

[13] K. Deb, S. Agrawal, A. Pratap, and T. Meyarivan, "A Fast Elitist Non-dominated Sorting Genetic Algorithm for Multi-objective Optimization: NSGA-II," in *International Conference on Parallel Problem Solving From Nature*, Berlin, Heidelberg, 2000, pp. 849–858. doi: 10.1007/3-540-45356-3_83.

[14] T. Peter, "Using Deep Learning as a surrogate model in Multi-objective Evolutionary Algorithms," Otto-von-Guericke-Universität, Magdeburg, 2018.

[15] C. Audet, J. Bigeon, D. Cartier, S. Le Digabel, and L. Salomon, "Performance indicators in multiobjective optimization," *Eur. J. Oper. Res.*, vol. 292, no. 2, pp. 397–422, Jul. 2021, doi: 10.1016/j.ejor.2020.11.016.

[16] K. Deb, "Multi-Objective Optimization Using Evolutionary Algorithms: An Introduction," p. 24, 2011.

[17] A. Charchalis, "Estimating The Main Dimensions Of The Ship's HuLL," *J. KONES Powertrain Transp.*, vol. 25, no. 2, 2018.

[18] C. E. Rasmussen and K. I. Williams, *Gaussian Processes for Machine Learning*. MIT Press, 2006. [Online]. Available: www.gaussianprocess.org/gpml

DOI: https://doi.org/10.29207/resti.v6i5.4248